Journal of Experimental Botany, Page 1 of 16
doi:10.1093/jxb/err025
This paper is available online free of all access charges (see http://jxb.oxfordjournals.org/open_access.html for further details)

Journal of Experimental Botany
www.jxb.oxfordjournals.org

RESEARCH PAPER

Poplar maintains zinc homeostasis with heavy metal genes *HMA4* and *PCS1*

Joshua P. Adams[1,*], Ardeshir Adeli[2], Chuan-Yu Hsu[1], Richard L. Harkess[3], Grier P. Page[4], Claude W. dePamphilis[5], Emily B. Schultz[1] and Cetin Yuceer[1]

[1] Department of Forestry, Mississippi State University, Mississippi State, MS 39762, USA
[2] USDA-ARS, Mississippi State, MS 39762, USA
[3] Department of Plant and Soil Sciences, Mississippi State University, Mississippi State, MS 39762, USA
[4] RTI International, Atlanta, GA 30341-5533, USA
[5] Department of Biology, Pennsylvania State University, University Park, PA 16802, USA

* To whom correspondence should be addressed. E-mail: jpa18@msstate.edu

Received 19 November 2010; Revised 28 December 2010; Accepted 7 January 2011

Abstract

Perennial woody species, such as poplar (*Populus* spp.) must acquire necessary heavy metals like zinc (Zn) while avoiding potential toxicity. Poplar contains genes with sequence homology to genes *HMA4* and *PCS1* from other species which are involved in heavy metal regulation. While basic genomic conservation exists, poplar does not have a hyperaccumulating phenotype. Poplar has a common indicator phenotype in which heavy metal accumulation is proportional to environmental concentrations but excesses are prevented. Phenotype is partly affected by regulation of *HMA4* and *PCS1* transcriptional abundance. Wild-type poplar down-regulates several transcripts in its Zn-interacting pathway at high Zn levels. Also, overexpressed *PtHMA4* and *PtPCS1* genes result in varying Zn phenotypes in poplar; specifically, there is a doubling of Zn accumulation in leaf tissues in an overexpressed *PtPCS1* line. The genomic complement and regulation of poplar highlighted in this study supports a role of *HMA4* and *PCS1* in Zn regulation dictating its phenotype. These genes can be altered in poplar to change its interaction with Zn. However, other poplar genes in the surrounding pathway may maintain the phenotype by inhibiting drastic changes in heavy metal accumulation with a single gene transformation.

Key words: Heavy metal, heavy metal transporter, phytochelatin synthase, poplar nutrition.

Introduction

Plant intake of essential heavy metals involves complex regulation that ensures adequate availability for various biochemical reactions while avoiding toxicity from excesses. Zinc (Zn) is one of the most prevalent essential heavy metals used by plants and plays important functions in >300 enzymes (Vallee and Falchuk, 1993; Coleman, 1998). However, excesses of Zn can be antagonistic to absorption of other essential elements due to transport and competition for storage space (Clemens *et al.*, 1999; Wang *et al.*, 2009*a*). Furthermore, metals can directly cause cellular damage through corruption of DNA integrity (Michaelis *et al.*, 1986; Hartwig *et al.*, 2002).

Plants appear to use the same basic mechanisms to regulate heavy metals. A common transporter associated with metal accumulation is an 1186-amino acid P-type heavy metal ATPase (HMA4) that plays a role in heavy metal transport efflux of many metals including Zn, copper (Cu), and iron (Fe) (Bernard *et al.*, 2004; Andres-Colas *et al.*, 2006). Furthermore, increases in *HMA4* expression have been shown to increase the tolerance to and accumulation of metals (Hanikenne *et al.*, 2008; Grispen *et al.*, 2011). Detoxification of heavy metals, especially non-essential heavy metals, is often attributed to post-translationally synthesized thiol-rich short metal binding proteins

Abbreviations: GSH, glutathione; PC, phytochelatin; PCS, phytochelatin synthase; PLSD, protected least significant difference; SR, stomata resistance; TR, transpiration rate.

termed phytochelatins (PCs) (Grill *et al.*, 1985), which are synthesized by phytochelatin synthase (PCS), which is one of the most frequently identified genes during a cDNA library screen for cadmium (Cd) tolerance (Bernard *et al.*, 2004). The role of PCs in heavy metal tolerance has been observed in many species including common velvetgrass (*Holcus lanatus*) (Hartley-Whitaker *et al.*, 2001), Azuki bean (*Vigna angularis*) (Inouhe *et al.*, 2000), wheat (*Triticum aestivum*) (Clemens *et al.*, 1999), Indian mustard (*Brassica juncea*) (Gasic and Korban, 2007), rapeseed (*Brassica napus*) (Mendoza-Cozatl *et al.*, 2008), and *Arabidopsis thaliana* (Vatamaniuk *et al.*, 1999) in which the metal binds with sulphur to form a large PC complex (Freedman *et al.*, 1989; Di Baccio *et al.*, 2005; Blum *et al.*, 2007). More recently, Zn excesses have been specifically shown to be mediated by an active role of PC production in *A. thaliana* (Tennstedt *et al.*, 2009).

Plants have evolved three main strategies for heavy metal interactions including indicators, excluders, and hyperaccumulators (Baker, 1981). These phenotypes are controlled by both the molecular constituency of the plant and its ecological patterns. Species such as *Oenothera biennis*, *Commelina communis*, *Silene vulgaris*, and *Rumex acetosella* are excluders at the molecular/physiological level that exclude metal (Wenzel *et al.*, 2003; Wei *et al.*, 2005), while celery (*Apium graveolens*), pakchoi (*Brassica chinensis*), and Chinese cabbage (*Brassica rapa*) exhibit signs of phytotoxicity at relative low ranges (e.g. <200 mg Zn kg^{-1}) (Long *et al.*, 2003) and exhibit an ecological excluder phenotype by not existing on metalliferous sites. A second indicater phenotype allows the plant to grow on elevated-metal sites by excluding intake of heavy metal excesses. This allows species to subsist on a range of sites with various metal loads. The final hyperaccumulating phenotype is exhibited by species, generally with small-biomass, such as *Thlaspi caerulescens* and *Arabidopsis halleri* that have found a niche in over-abundant metal environments (Chaney *et al.*, 2000) and can accumulate as much as 10-fold the Zn relative to non-hyperaccumulating species (Lasat *et al.*, 1998). High-biomass tree species, such as poplar, are generally thought to have a metal indicator phenotype with Zn accumulation in stems occurring at low levels [<200 mg kg^{-1} (Sebastiani *et al.*, 2004; Laureysens *et al.*, 2005)] and at extremely high levels [>3000 mg kg^{-1} (Pierzynski *et al.*, 2002; Unterbrunner *et al.*, 2007)] depending on the site. However, the specific manner by which poplar regulates heavy metal accumulation is unknown.

The mechanisms regulating plant–zinc interactions have been extensively studied for small, annual species especially in species with hyperaccumulating phenotypes (e.g. *T. caerulescens*). However, these mechanisms are relatively unexplored in large, perennial species such as the high biomass *Populus trichocarpa*, which is the model forest species. The overall objective of this study is to elucidate the effect of poplar heavy metal genes *HMA4* and *PCS1* as they relate to Zn interaction. This is first accomplished through genomic comparisons with phylogenetic analysis allowing gene identification and assessment of evolutionary relationships between species with varying phenotypes. Quantification of transcript abundance modulations in poplar relative to other species further delineates how poplar interacts with Zn. Finally, the effect on the phenotype and physiology of poplar is quantified after overexpression of *HMA4* and *PCS1*. The results of these studies lead to a further understanding of the poplar phenotype and are a first step towards identification of avenues for creation of a hyperaccumulating poplar phenotype for use in phytoremediation.

Materials and methods

Phylogenetic and pathway analyses

Phylogenetic and pathway analyses were used to identify the best *HMA4* and *PCS1* homologues in poplar and place them in both an evolutionary and a pathway context. Poplar genes with sequence homology to *TcHMA4* and *TcPCS1* in *T. caerulescens* were retrieved from keyword searches, eudicot gene cluster searches, and sequence blasts (i.e. BlastP) of the NCBI database (www.ncbi.nlm.nih.gov) and the Phytozome v 5.0 database (www.phytozome.net/poplar.php), which includes the *P. trichocarpa* genome v 2.0. Transcript sequences were retrieved and imported into MEGA 4 (Tamura *et al.*, 2007), translated into amino acid residues, and aligned with ClustalW (Thompson *et al.*, 1997) using the Gonnet protein weight matrix. Using the maximum composite likelihood substitution model, a phylogenetic tree was generated via the neighbor-joining method with bootstrapping (1000 replicates). Each tree was rooted on a rice (*Oryza sativa*) orthologue annotated as a functional ZIP gene. This process was conducted for both *T. caerulescens* genes and resulted in two independent phylogenic trees. HMA4 and PCS1 homologues were further analysed for similarity by comparing predicted HMA4 transmembrane helices using TMMTOP (Tusnady and Simon, 1998) and by counting conserved cysteine motifs found in PCS (Clemens, 2006).

Pathway analysis was conducted to search for a broader network of genes with which *HMA4* and *PCS1* may interact to affect Zn regulation. A heavy metal pathway was identified using a microarray dataset of overexpressed genes from heavy metal-hyperaccumulating *A. halleri* relative to homologues in non-hyperaccumulating *A. thaliana* (Becher *et al.*, 2004) and a study comparing heavy metal-hyperaccumulating *T. caerulescens* and non-hyperaccumulating *Thlaspi arvense* (Hammond *et al.*, 2006). Transcripts differentially expressing >2.0-fold or <0.5-fold were selected (respectively, 499+5985=6484 transcripts) and imported with their respective poplar expression ratios (detailed in the following section) into Pathway Studio v 7.0 (Ariadne Genomics, Rockville, MD, USA). Genes were selected from the imported transcripts that were related to gene ontology (GO) groups that included cation, Zn, and Cd interactions. From these selections, a pathway was established using ResNet 2.0 database (Ariadne Genomics), which included transcripts not necessarily in the previous microarray studies. A section of the large pathway was selected that contained transcripts shown through previous studies to be related to physiological traits associated with plant–metal interactions. The final pathway was tested with Fisher's exact test to determine whether the genes in this condensed pathway significantly enriched specific GO annotation groups. Poplar homologues for the genes were found by blasting (i.e. BlastP) this protein sequence into the poplar database.

Zn challenge assays and nutrient/transcript analyses

Poplar plants were established and assayed with varying Zn concentrations for transcript and nutrient analyses. Six- to eight-inch

(150–200 mm) woody stems were harvested from field-grown *P. trichocarpa* cv. Nisqualy in early spring, dipped in Hormex© rooting powder #16 (Hollywood, CA, USA), planted in moist soil, and grown in a greenhouse from early March to May. The greenhouse provided for temperature control through limiting ambient temperature highs to no more than 32 °C; however, there was no humidity control and no supplementary lighting. A water misting system was used that misted plants and soil surface every 5 min for 30 s at a rate of 15 l h^{-1}. Plants were then transplanted into sterile sand in a 12.25 cm pot with an attached water-catching basin and supplemented with Hoagland's nutrient solution (1 μM Zn) every 2 d for 8 d. This application regime was chosen based on preliminary tests that showed that nutrient application every 2 d prevented excess solution leaching while providing adequate nutrients for the plant. Plants were then randomly assigned to three metal treatments and two harvesting times with each treatment-by-harvest time combination containing eight replications. The three Zn treatments were an unmodified Hoagland's solution containing 1 μM $ZnSO_4$ (control) and Hoagland's solution supplemented with an additional 10 μM or 1 mM $ZnSO_4$. The harvest times were 24 h and 48 h (Kohler *et al.*, 2004) after application of nutrient solution. At harvest, the plants were washed, and leaves, stems (all above-ground tissues excluding leaves), and roots were frozen separately in liquid nitrogen, and stored in a –80 °C freezer.

Poplar transcript abundance was compared across metal treatments. RNA was extracted from tissues using a hot borate RNA extraction method (Wan and Wilkins, 1994) followed by treatment with on-column DNase I treatment (Promega, Madison, WI, USA) and RNA clean-up via RNeasy Plant Mini Kit (Qiagen, Valencia, CA, USA). RNA (1 μg) was reverse-transcribed using M-MLV reverse transcriptase (Promega). Transcripts were analysed via qPCR using Power SYBR-Green (Applied Biosystems, Carlsbad, CA, USA). Ubiquitin transcript (*UBQ*) amplification was used as an internal control for both qPCR analyses (Infante *et al.*, 2008). Primers used in Power SYBR-Green reactions were verified for specificity via ABI Prism dissociation curve analysis software and also by separating the PCR products by electrophoresis on a 1% agarose gel. All primers used throughout this study were preliminarily tested for specificity before use and can be found in Supplementary Table S1 (Supplementary data available at *JXB* online). Amplification reactions were performed using ABI 7500 Fast Real-Time PCR System (Applied Biosystems) relative transcript quantification. Each reaction mixture contained 0.5 μl of cDNA template, 5.0 μl of SYBR-Green Master Mix, 0.25 μl of both 10 μM primers, and 4.0 μl of ddH_2O. The qPCR programme consisted of an initial incubation (95 °C for 10 min) followed by 35 cycles of 95 °C for 15 s and 60 °C for 1 min. Each reaction was independently repeated at least three times. Standard curves were constructed using serial dilutions of cDNA. Transcripts were analysed by using threshold amplification points (C_t values) with the standard curves to calculate transcript concentration. Subsequently, the ratio of target transcript concentration to *UBQ* transcript concentration was calculated for each transcript. These values were log transformed and analysed with a mixed-effect general linear model using SAS v 9.1 (SAS Institute, Cary, NC, USA) in which there was a fixed metal effect, a fixed day co-variant effect, and a random biological (plant) effect.

Zn and other nutrients in poplar were compared across the Zn treatments. Remaining tissues from the metal challenge were analysed for nutrient concentrations. At least three samples of each tissue (root, stem, and leaf) at each metal exposure level (1 μM, 10 μM, and 1 mM) were used. Samples were taken from –80 °C storage, dried for 48 h at 50 °C, and ground into a fine powder with a mortar and pestle. Samples were then processed with a dry ash procedure (Isaac, 1983) to obtain nutrient concentrations [Ca, Cu, Fe, potassium (K), magnesium (Mg), sodium (Na), phosphorus (P), and manganese (Mn) mg kg^{-1}] and with a nitric acid extraction procedure to obtain Zn concentrations (Ebbs and Kochian, 1998). All nutrients from the leaf, stem, and root tissues were determined spectrophotometrically using an inductively coupled plasma (ICP) emission spectrophotometer (Thermo Jarrel Ash Iris Advantage ICP, Houghton, MI, USA). A mixed general linear model was used to compare the metal concentrations between the fixed tissue and metal exposure effects and the random biological (plant) effect using SAS v 9.1. Nutrient trends in accumulation and compartmentalization were compared by rescaling all nutrient concentrations and calculating Euclidean distances between each tissue, sample time, and Zn treatment from which a dendrogram was built using R software (R Development Core Team, 2008).

Overexpression of PtPCS1 *and* PtHMA4 *genes in poplar*

PtPCS1 and *PtHMA4* were isolated, modified with an overexpression promoter, and transformed back into poplar plants. Total RNA was extracted from *P. trichocarpa* cv. Nisqualy using RNeasy Plant Mini Kit. Total RNA (1 μg) was reverse-transcribed using M-MLV reverse transcriptase (Promega). Forward and reverse primers were designed based on each database cDNA sequence (Supplementary Table S2 at *JXB* online). The full-length coding sequence of each gene was amplified using PCR with *Pfu* DNA polymerase (Stratagene, La Jolla, CA, USA) using a three-step (94 °C for 20 s, 60 °C for 20 s, and 72 °C for 145 s) 30-cycle programme. PCR products were separated on a 1% agarose gel, extracted, cloned into the pGEM-T Easy vector (Promega), and sequenced with a CEQ 8000 Genetic Analysis System (Beckman-Coulter, Fullerton, CA, USA).

Additional restriction site sequences (Supplementary Table S2 at *JXB* online) were designed for the termini of each gene and added using a second PCR amplification reaction. This PCR reaction used the cloned gene as the template, primer pairs (with added restriction sites), and *Pfu* DNA polymerase in a 30-cycle programme (94 °C for 20 s, 60 °C for 20 s, and 72 °C for 145 s). Each PCR product was purified from agarose gel, cloned into pGEM-T Easy vector, and resequenced to ensure absence of sequence polymorphisms. Each gene construct was digested with appropriate restriction enzymes and cloned into the binary vector pBI121 (Clontech, Palo Alto, CA, USA). In both constructs, the gene replaced the β-glucuronidase (GUS) reporter gene downstream of the cauliflower mosaic virus (CaMV) 35S constitutive expression promoter and upstream of the nopaline synthase promoter (NOS) terminal sequence. The binary vectors P_{35S}:*PtPCS1* and P_{35S}:*PtHMA4* were transformed into *Agrobacterium tumefaciens* strain C58, which subsequently was used to transform the hybrid poplar clone INRA 717-1B4 (*Populus tremula*×*Populus alba*).

Poplar transformation was performed using an established transformation procedure (Han *et al.*, 2000). Between 5 and 10 independent lines were generated and transgene insertion was confirmed with genomic PCR using the respective gene's forward primer and the NOS terminal reverse primer. Expression of the transgene was tested with qPCR using the previously detailed procedures.

Zinc challenge of plants overexpressing PtHMA4 *and* PtPCS1

Overexpression lines were assayed with various concentrations of Zn to assess gene function. An average overexpressing poplar line of both constructs and two controls (wild-type and pBI101 lines) were used to assay rooting ability as a proxy for tolerance in elevated Zn conditions (Gasic and Korban, 2007). The pBI101 poplar line contained the empty vector pBI101 with no promoter (BD Biosciences, Mountain View, CA, USA). Stem segments ~2.5 cm long were excised from plants grown in Magenta boxes with 39.5 cm^2 of growing area (Plantmedia, Dublin, OH, USA) and half-strength Murashige and Skoog medium with 0.8% agar. These segments were stripped of leaves and inserted into media containing unmodified Hoagland's Solution with three different Zn concentrations [1 μM (control metal concentration), 10 μM, and 1 mM $ZnSO_4$] and 0.8% agar. Thus, a nested 3 (metal treatment)

by 4 (line) factorial design with four replications was used in which lines were tested across three metal concentrations, and five line replications were nested within each plate. They were grown for 30 d in growth chambers with environmental conditions: 8/16 h (night/day) day length, 25 °C, and 45% relative humidity. Throughout the course of the study, rooting emergence, leaf emergence, and time to rooting emergence were recorded and root weight was measured after completion of the 30 d.

The three selected *P_{35S}:PtPCS1* lines, representing high, medium, and low overexpression levels, and two control lines were assayed for Zn accumulation. Twelve plants from these three lines and two control lines were grown for 2–4 months from March to July in potting soil under controlled greenhouse conditions as previously described. Each plant was transplanted into sterile, inert sand substrate in a 12.25 cm pot with an attached water-catching basin and supplemented with Hoagland's Solution, which was renewed every other day for 1 week prior to starting the metal assay. Again, a water misting system that misted plants and soil surface every 5 min for 30 s at a rate of 15 l h^{-1} was used.

These plants were randomly assigned to the metal assay using a 4 (lines) by 3 (Zn treatment) factorial design. Four plants from each line were randomly assigned to three Zn levels. The Zn treatments were conducted by applying 25 ml of three different rates of $ZnSO_4$ as a supplement to the unmodified Hoagland's Solution every 2 d. $ZnSO_4$ was applied at a concentration of 1 μM, 1 mM, and 10 mM. The 10 mM concentration was chosen to represent an unnatural, excessive concentration to ensure plant stress. Thus, at the completion of the study, the plants in the 10 mM treatment were exposed to ~1078 mg of $ZnSO_4$. Remaining in the greenhouse, plants were grown for 30 d during July and August with no supplemental lighting. Throughout the study, plants were visually inspected and compared with controls for phytotoxicity symptoms, such as leaf coloration and necrosis. Also, at 12:00 pm on days 0, 10, 20, and 30, the second fully developed leaf from the tree stem apex was measured for stomata resistance (SR) and transpiration rate (TR) using a Li-Cor 1600 SteadyState Porometer (Lincoln, NE, USA) on each plant. At each sampling time, environmental conditions included 45–60% relative humidity and a clear sky. At day 30, the whole plants were harvested, separated by tissue, and dried for 48 h at 50 °C, measured for dry weight, and analysed for heavy metal content as previously described. Porometer measurements were analysed using a general linear model procedure corrected for compound symmetry time correlations. Heat maps of the measurements were generated by constructing an artificial matrix of variable combinations including all times between 0 d and 30 d and all Zn concentrations between 0 μM and 1 mM. A loess model was used to predict TR and SR ratios for each point in the constructed matrix. Dry weight data and nutrient analysis data were evaluated using a fixed-effect general linear model and protected least significant difference (PLSD) using SAS v 9.1. Nutrient values were rescaled, Euclidean distances were calculated over each tissue, Zn treatment, and line, and a dendrogram was built using R software (R Development Core Team, 2008). Nutrient data from each line were merged with transcriptional data from each line and a general linear model was used to test the effect of *PtPCS1* on metal accumulation. A three-dimensional surface was constructed to represent the changes across *PtPCS1* expression, Zn treatment, and metal (Zn, Cu, and Fe) accumulation. An artificial matrix was constructed across the range of all combinations of expression and Zn treatment. Local regression was used to predict metal accumulation for each point and predictions were then plotted.

Results

Poplar contains heavy metal-related genes

Two genes closely related to *TcHMA4* and *TcPCS1* were identified in poplar and are part of a broader pathway of genes. Poplar genes *POPTR_0006s07650.1* and *POPTR_0014s18420.1* share sequence homology with two established *T. caerulescens* genes, *TcHMA4* and *TcPCS1*, respectively. Poplar has 11 *HMA4* genes that are more closely related to *TcHMA4* than the rice outgroup. However, *HMA*(1) (*POPTR_0006s07650*) was more closely related to *TcHMA4* than the other 10 genes (Fig. 1A). This transcript (*PtHMA4*) was the best hit during the protein BLAST and was the only poplar gene that was in the clade close to *HMA4* genes of species in the Brassicaceae family. Predicted topologies of the proteins show a wide array of transmembrane loops from five to nine (Supplementary Table S3 at *JXB* online). The most conserved area is among the *HMA*s of the mustard species with nine transmembrane loops. The closest poplar homologue only has seven loops. The PCS phylogeny only included two possible poplar homologues. The locations of these two genes in the tree indicate that *PCS1*(1) (*POPTR_0014s18410.1*) is closest to *TcPCS1* (Fig. 1B). However, *PCS1*(2) (*POPTR_0014s18420.1*) was the best *TcPCS1* BLAST hit in the poplar genome, had the greatest percentage protein identity (67% versus 58%), had the same number of conserved cysteine motifs, and thus, was selected as the PCS homologue.

In the pathway analysis, 6484 transcripts from previous studies represented 1545 GO annotation groups. Groups related to heavy metals included cation transport, cation transmembrane transporter activity, Cd ion transport, Cd ion transmembrane transport, Zn ion transport, Zn-mediated transmembrane transport, Zn ion transporter activity, and Zn ion binding. The condensed pathway (Supplementary Table S4 at *JXB* online) contained five transcripts that contributed significantly to ATPase activity, Cd ion transmembrane transporter activity, Zn ion transmembrane transporter activity, and Zn ion transport with $P<0.05$ for these GO annotation groups (Supplementary Table S5 at *JXB* online). Two genes in the pathway were *PtHMA4* and *PtPCS1*. The other genes included two related to ATPase activity (*APY2* and *AHA3*) and one dehydrase (*ELI3-1*).

Poplar adapts to changes in zinc concentration

Poplar reacted to Zn changes both in metal accumulation and in transcriptional abundance of the two identified genes, *PtHMA4* and *PtPCS1*, and their broader interacting pathway. Metal and nutrient accumulation by tissue, day, and Zn treatment demonstrate that localization of most nutrients occurs in poplar roots or leaves (Fig. 2A; Supplementary Table S6 at *JXB* online), while stems had relatively depressed loads of all nutrients except for Na, P, and K. Leaves also had very high concentrations of these three nutrients as well as Mg, Mn, and Ca, causing these six nutrients to cluster together. The other three nutrients, Zn, Cu, and Fe, cluster together and were primarily concentrated in root tissues. Within the cluster containing Zn, differences were seen between Zn and the other two metals. Zn accumulation in these wild-type poplars was

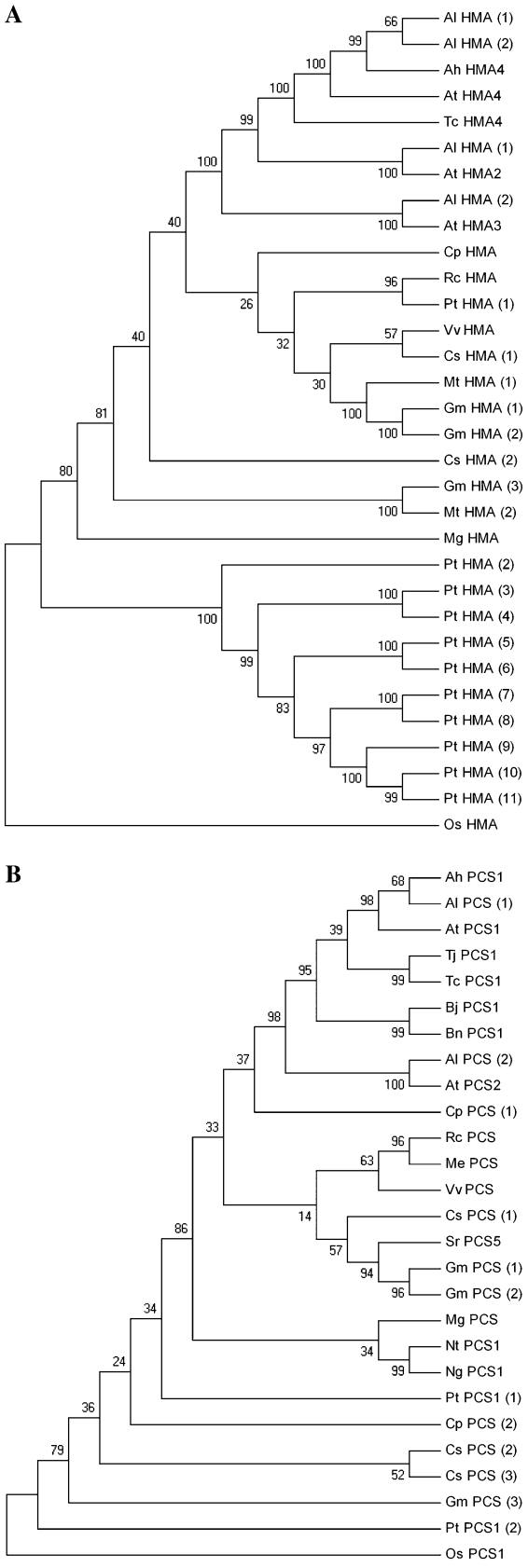

Fig. 1. Phylogenetic tree of (A) TcPCS1-like and (B) TcHMA4-like sequences. Bootstrap percentages (n=1000) are located at nodes. Each tree contains a gene from the hyper-accumulator *T. caerulescens* (i.e. *TcHMA4* and *TcPCS1*). Accession numbers corresponding to the gene names are located in Supplementary Table S3 at *JXB* online. Species include: Ah, *A. halleri*; Al, *Arabidopsis lyrata*; At, *A. thaliana*; Tj, *Thlaspi japonicum*; Tc, *T. caerulescens*; Bj, *B. juncea*; Bn, *B. napus*; Cp, *Carica papaya*; Rc, *Ricinus communis*; Me, *Manihot esculenta*; Vv, *Vitis vinifera*; Cs, *Cucumis sativus*; Sr, *Sesbania rostrata*; Gm, *Glycine max*; Mt, *Medicago truncatula*; Mg, *Mimulus guttatus*; Nt, *Nicotiana tabacum*; Ng, *Nicotiana glauca*; Pt, *Populus deltoides*; and Os, *Oryza sativa.*

significantly (P<0.001) affected by plant tissue type (leaf, stem, and root) and by Zn exposure concentration (Fig. 2B), but not affected (P=0.85) by exposure time (24 h and 48 h). Greatest accumulation differences occurred in roots under 1 mM Zn exposure, which accumulated more Zn than the other treatments. These differences decreased in the aerial tissues and between the 1 μM and 10 μM Zn exposures. An opposing trend was observed with closely related Cu. There was a significant tissue–Zn treatment interaction effect (P=0.005), in which high Zn levels negatively affected Cu absorption by roots (Fig. 2C).

Preliminary transcript assays in leaves mirrored the insignificant Zn accumulation changes in the leaf and were not studied further. *PtHMA4* and *PtPCS1* were assayed in stem and root tissues. Stem tissues had significant *PtHMA4* and *PtPCS1* changes in transcript abundance across the Zn gradient (P<0.001) (Fig. 2D; Supplementary Table S7 at *JXB* online). These differences were greatest between the 1 mM treatment level and lower 1 μM and 10 μM treatments. The transporter *PtHMA4* had a 0.63-fold decrease in expression between the highest and lowest concentrations with greatest abundance in roots (2.4-fold the abundance in stems). *PtPCS1* was also significantly decreased when exposed to 1 mM Zn with a 4.8-fold drop in transcript abundance in stems. Overall, stems contain the highest *PtPCS1* abundance with an average 17.2 times the amount in roots.

In roots, where metal differences were greatest, three additional genes identified through the pathway analysis were analysed. Overall, the transcript abundance pattern was the same as that seen in stems in which expression decreased significantly with increases in Zn exposure (Fig. 2E). The notable exception was *PtPCS1*, which did not have a significant (P=0.18) increase as metal concentration changed.

Overexpression of HMA4 *and* PCS1 *affect poplar–Zn interaction during early development*

Altering expression of *PtHMA4* and *PtPCS1* affected Zn interaction with regard to tolerance and accumulation. Independent lines of poplar containing *PtPCS1* (Fig. 3A) and *PtHMA4* (Fig. 3B) under constitutive control were successfully created. The connection between *PtPCS1* and *PtHMA4* in Fig. 2D was quantitatively investigated for a transcriptional link via qPCR using tissues from both

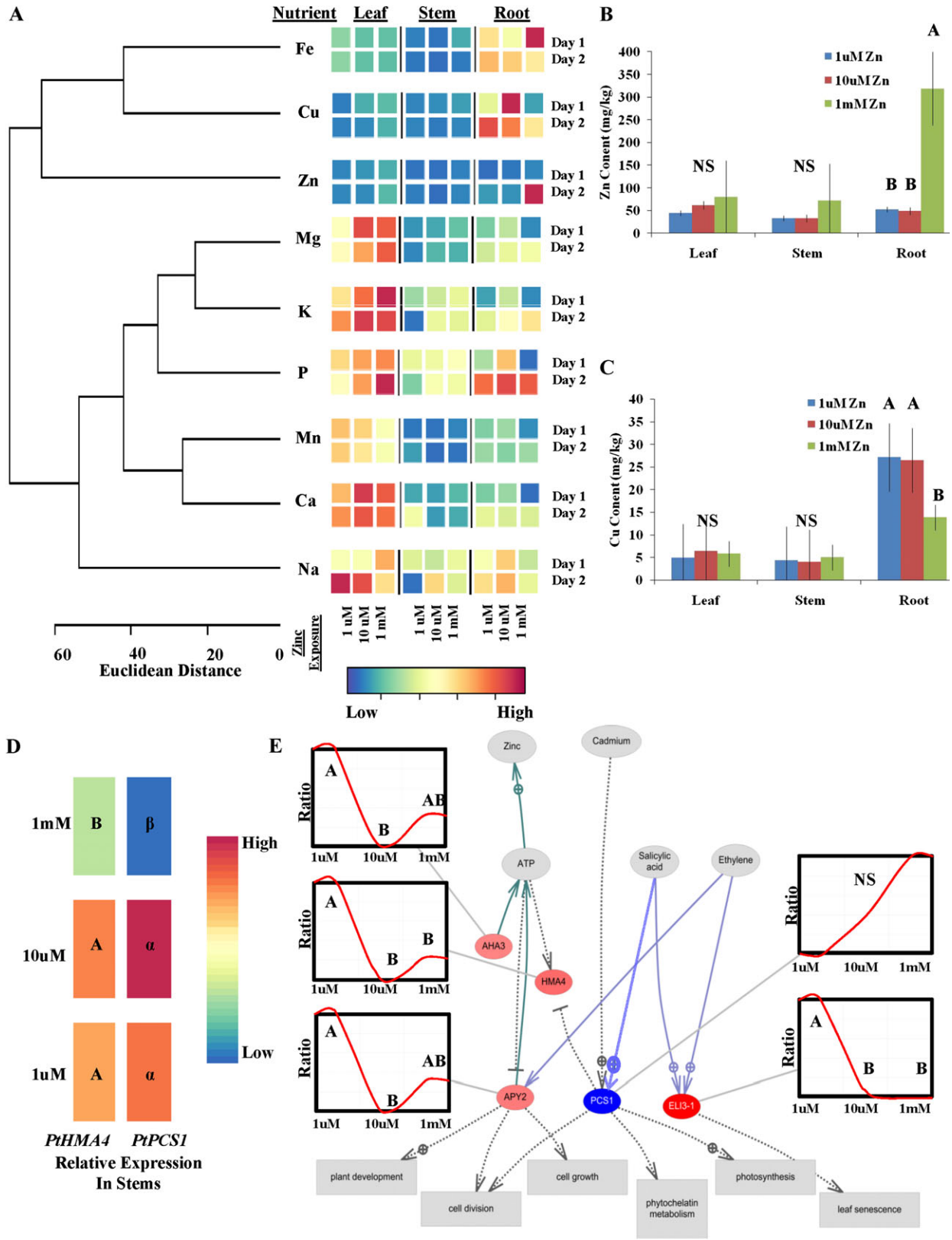

Fig. 2. Nutrient accumulation of *P. trichocarpa* cv. Nisqualy sampled under Zn treatments of 1 μM, 10 μM, and 1 mM (n=59). (A) Relationships based on average Euclidian distance of nutrient accumulation across 2 d, metal exposure, and tissue type and their relative concentrations. (B) Zn and (C) Cu accumulation in root, stem, and leaf tissues across both sampling periods. (D) Transcriptional abundance changes of *PtHMA4* and *PtPCS1* in stem tissue where ratios of gene/ubiquitin, ranging between 1.6- and 45.4-fold, are indicated by colour. (E) The pathway represents the connections of these same two genes and closely connected poplar genes to external stimuli and physiological effects with red to blue coloration denoting relative, high to low, magnitude change in gene/ubiquitin

constructs and controls. As expected, *PtPCS1* expression was significantly (P=0.02) higher (3.8-fold) in the P_{35S}:*PtPCS1* lines relative to either the P_{35S}:*PtHMA4* lines or the controls (Fig. 3C). Expression of *PtPCS1* in the P_{35S}:*PtHMA4* construct was not significantly different from the control plants. *PtHMA4* expression among the two lines and control behaved differently. As expected, there was an overall difference (P=0.03) with *PtHMA4* expression levels in the P_{35S}:*PtHMA4* construct nearly 21 times that found in the wild-type plants. However, the P_{35S}:*PtPCS1* construct had elevated *PtHMA4* levels as well. The P_{35S}:*PtPCS1* construct expressed *PtHMA4* an average seven times more than the control plants, and was statistically different from neither the P_{35S}:*PtHMA4* lines nor the wild-type lines. This co-increase in both transcripts may indicate that *PtPCS1* has a downstream positive effect on *PtHMA4* in poplar.

Controls and Line 1 of both the P_{35S}:*PtPCS1* and P_{35S}:*PtHMA4* constructs were assayed to study early development. After only a few (3–5) days, visual negative effects, including reduced stem or root development and chlorosis of leaves, were evident for all lines exposed to 1 mM Zn (Fig. 3D). After 30 d, rooting was rare for any plantlets exposed to the 1 mM Zn treatment (~2% across all lines), and those few that did root only rooted in the final days of the study. Therefore, analysis was only conducted on the 1 μM and 10 μM Zn concentrations. Visual differences were slightly evident between the 1 μM and 10 μM Zn treatments with plants receiving the lower concentrations having healthier, darker green leaves. P_{35S}:*PtHMA4* was visually the healthiest with dark green leaves and vibrant, spreading roots. Wild-type plants were not as vigorous but grew slightly better than the P_{35S}:*PtPCS1* lines. P_{35S}:*PtPCS1* plants did survive and root, but their roots were generally smaller and were less apt to spread.

Leaf emergence from the stem segment supports the visual differences seen between lines. The percentage per plate of stems that formed leaves was significantly different (P=0.003) between lines, with P_{35S}:*PtHMA4* having the greatest percentage (89%) and P_{35S}:*PtPCS1* and controls (28–30%) not exhibiting any significant difference (Fig. 3E). Rooting percentage was significantly affected by an interaction (P<0.001) between Zn concentration and lines. Rooting percentage was stable between the two metal concentrations (Fig. 3F). However, the two transgenic lines showed opposing Zn effects in which the P_{35S}:*PtPCS1* line had a large percentage increase (47%) at the higher Zn concentration and P_{35S}:*PtHMA4* line had a large decrease (32%) at the higher concentration. Plantlets that rooted did so at significantly different times by line (P=0.01) (Fig. 3G). On average, the P_{35S}:*PtPCS1* line and controls (19–21 d) rooted at the same time, while the P_{35S}:*PtHMA4* line rooted much earlier (13 d).

Overexpressed PCS1 *increases Zn concentration in poplar*

The metal assay on older plants was conducted on three lines of P_{35S}:*PtPCS1*. Lines 1, 2, and 3 were selected to represent respectively medium, low, and high concentrations of the overexpressed *PtPCS1* (Fig. 3A). In this longer-term study, both transgenic and control poplars were resilient to 1 mM and 10 mM Zn exposure with no mortality. This is in contrast to the near complete suspension of development (i.e. rooting and leafing) at 1 mM in the rooting study. Still, biomass partitioning was affected by line and Zn concentration exposure independently (Supplementary Table S8 at *JXB* online). The effect on partitioning was not observed in the root-to-stem ratio (P=0.169), but was significant with regard to the root-to-(stem+leaf) ratio (P=0.002) indicating that a shift was occurring in foliar weight (Fig. 4A). In this case, the ratio for the control plants was significantly reduced compared with all the transgenic lines; thus, P_{35S}:*PtPCS1* lines had less foliar biomass relative to the weight of other tissues. Zn exposure affected both ratios significantly [P=0.05 and 0.04 for root-to-stem and root-to-(stem+leaf), respectively] (Fig. 4B). Since both ratios were significantly affected by metal concentration, there was a decrease in root biomass growth at the elevated Zn concentrations.

The physiological effect evident during visual inspection was a change in leaf and stem coloration in which plants exposed to high Zn levels began to express brown/red coloration in foliage compared with the normal green (Fig. 4C) However, these differences were only visually evident among the Zn treatments and not among lines. Thus, leaf differences among lines and levels of Zn exposure were quantified by measuring leaf SR and TR through the course of the assay. Both SR and TR were significantly affected by an interaction of line and concentration (P=0.033 and 0.024, respectively). SR change fluctuated the least across time and Zn concentration in Line 3 and the control (Fig. 4D). These showed only a slight increase at the highest Zn exposure. By the end of the study there was less variation in Lines 1 and 2. TRs among the control plants were low and stable across both Zn concentration and time. However, the three lines of P_{35S}:*PtPCS1* behaved

ratio (overall range 1.0–37.5) across treatments, respectively. Sample size of all transcript analyses was n=9 for each day–tissue–treatment combination. Connections in the pathway represent the following: dotted black line, regulation; purple solid line, expression; and solid turquoise line, molecule transport. Abbreviations and poplar identifications are: PCS1, phytochelatin synthase 1 (POPTR_0014s18420.1); APY2, apyrase 2 (POPTR_0013s05040.1); ELI3-1, elicitor-activated gene 3 (POPTR_0006s21360.1); AHA3, *Arabidopsis* H(+)-ATPase 3 (POPTR_0006s00770.1); HMA4, heavy metal ATPase4 (POPTR_0006s07650.1). Letters in the graph section represent Fisher's PLSD mean separation where differing letters represent significantly different means at the 0.05 level. NS, no significant difference.

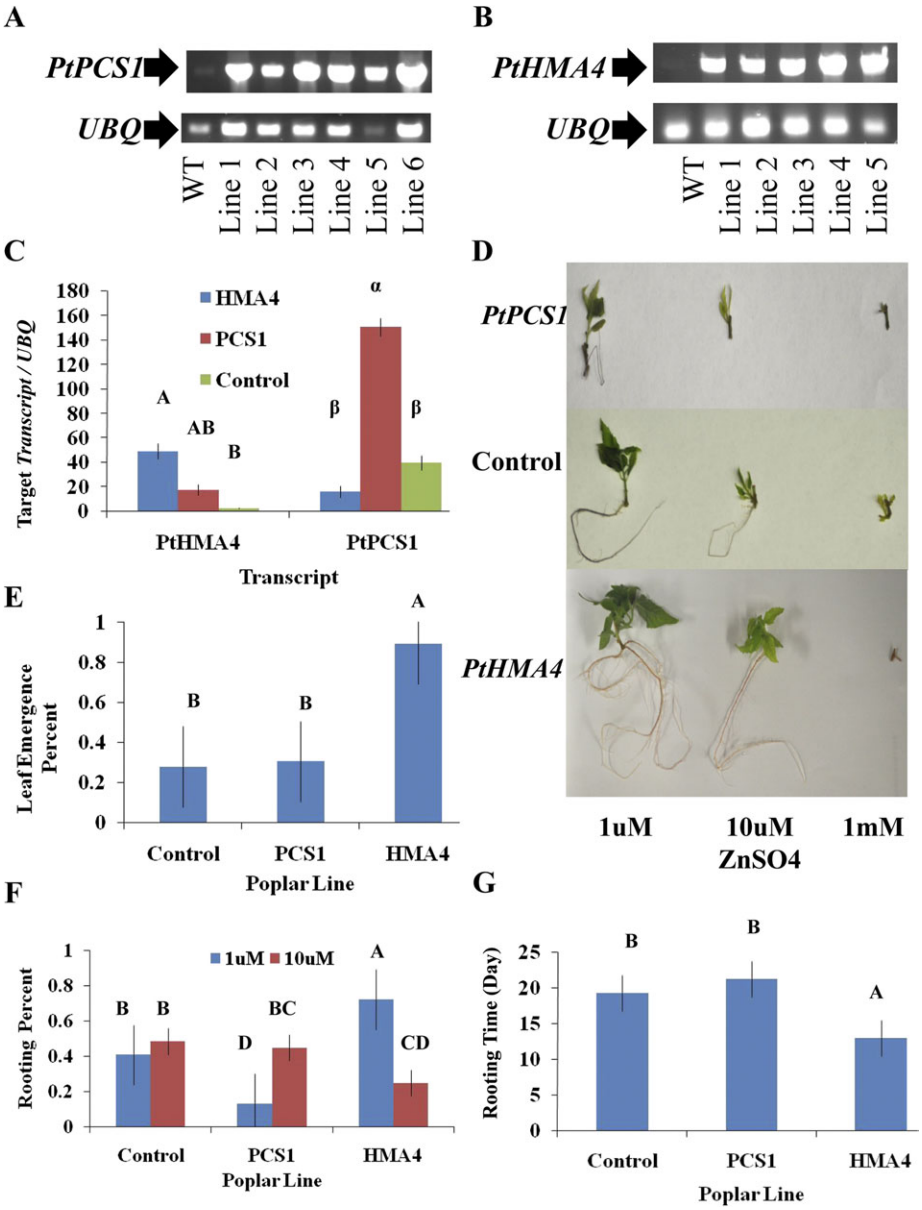

Fig. 3. P_{35S}:*PtPCS1* and P_{35S}:*PtHMA4* effects on transcript abundance and early development of propagules. Expression of (A) *PtPCS1* and (B) *PtHMA4* overexpression lines were assayed with RT-PCR using 28- and 30-programme cycles, respectively. (C) Transcriptional abundance of *PtPCS1* and *PtHMA4* was tested under control (1 μM) conditions with pooled control lines (three plants from pBI101 and wild-type 717 each) and three plants each from both P_{35S}:*PtPCS1* lines and P_{35S}:*PtHMA4* lines. (D) Plantlets of control, P_{35S}:*PtPCS1*-Line 1, and P_{35S}:*PtHMA4*-Line 1 were placed in growth media containing 1 μM, 10 μM, or 1 mM Zn for 30 d (n=244). The percentage of stems that had (E) leaf emergence across the significant (P=0.003) metal treatment effect after 30 d, (F) root emergence across the significant metal (1 μM and 10 μM)–line interaction effect (P<0.001) after 30 d, and (G) the days taken for root emergence across Zn concentration for the significantly (P=0.01) different lines. Letters in the graph section represent Fisher's PLSD mean separation where differing letters represent significantly different means at the 0.05 level. NS, no significant difference.

differently (Fig. 4E). TRs for Line 1 generally increased at low levels of Zn exposure while Lines 2 and 3 exhibited decreased TRs.

Exposure to 30 d of elevated Zn affected poplar's accumulation of nutrients and highlighted accumulation differences between the lines and controls. The accumulation patterns of other nutrients across tissues and treatments was different from Zn accumulation patterns indicated by the dendrogram showing Zn as an outgroup (Fig. 5A). Generally, increases in Zn exposure were antagonistic to accumulation of other nutrients. The length of the assay (30 d) as well as the higher concentrations used also created a different pattern of localization compared with the 48 h assay (Fig. 2A), in which all nutrients accumulated primarily in leaves and, to a lesser extent, roots (Supplementary Table S9 at *JXB* online).

In root, stem, and leaf tissues, Zn exposure significantly affected accumulation (P<0.001 for all tissues). However,

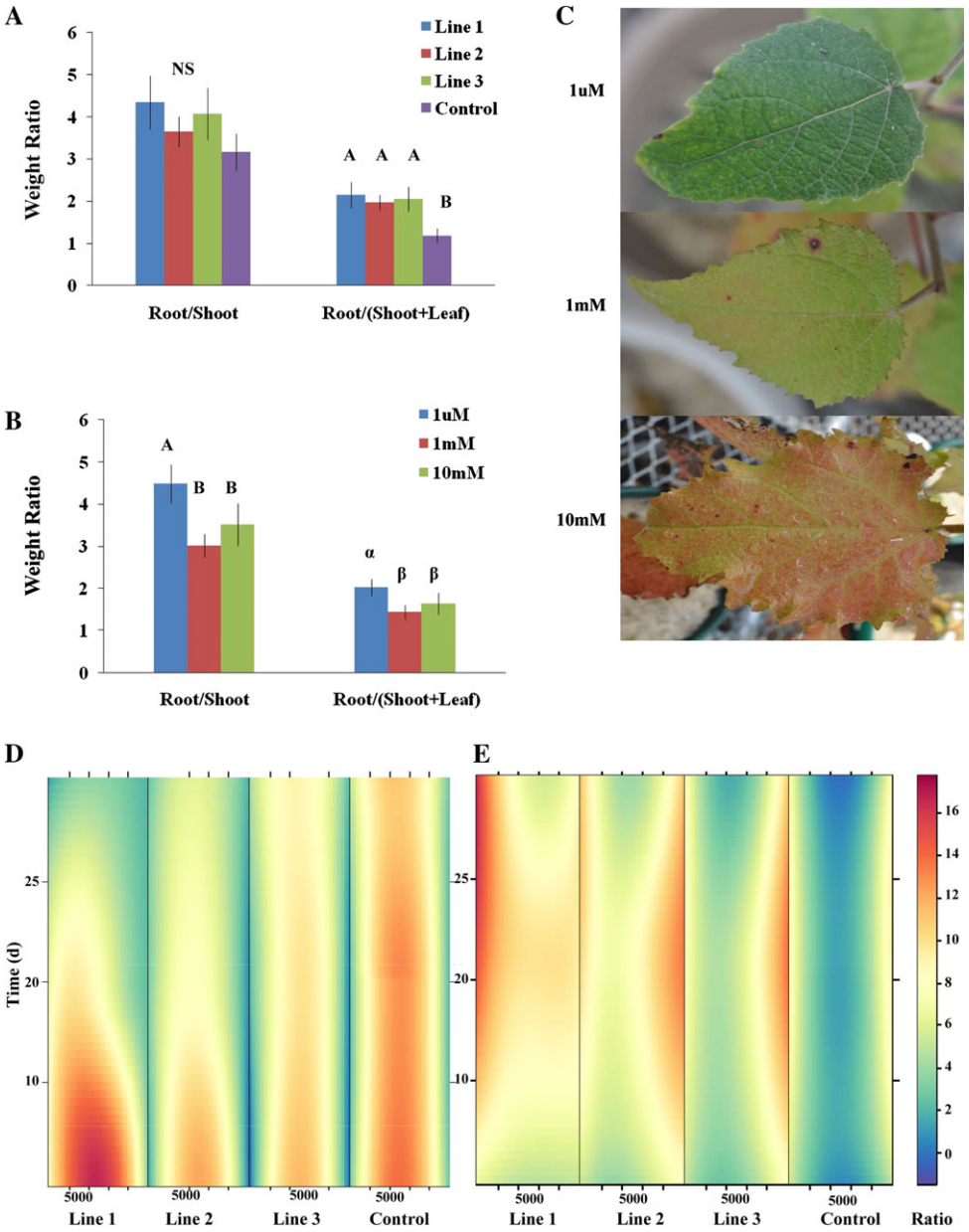

Fig. 4. The physiological impact of metal treatments on P_{35S}:*PtPCS1* transgenic lines and controls (overall n=60). This includes the independent effects of line and Zn treatment on dry tissue weight ratios for (A) tested lines across metal treatment and (B) Zn treatments across lines after harvest at 30 d. (C) Effect of metal exposure on poplar leaves at 30 d. (D) Stomatal resistance (s cm^{-1}) and (E) transpiration (μg cm^{-2} s^{-1}) ratio [measurement at time x/ measurement at time (x–1)] projections across metal exposure and study duration for each line. Projections were made using loess model (TR/SR=concentration×time+lines) predictions for each point of an artificial grid with the x-axis metal exposure concentration ranging from 0 μM to 10 000 μM. Letters in the graph section represent Fisher's PLSD mean separation where differing letters represent significantly different means at the 0.05 level. NS, no significant difference.

while a line effect was not present in the root tissues (P=0.28), in both stem and leaf tissues there was an interaction effect between line and Zn concentration (P=0.026 and 0.023, respectively). This interaction effect only led to actual statistical differences between lines at the highest exposure concentration (i.e. 10 mM Zn) with Line 3 accumulating only 188 mg kg^{-1}, which is less than half the accumulation of either the control or the other two lines (Fig. 5B). Differences in leaf Zn accumulation among lines were also evident (Fig. 5C). Again, the lowest exposure level (1 μM Zn) led to no differences between lines. However, in leaf tissue, lines exhibited differences under both elevated concentration treatments. Line 1 accumulated the highest concentrations of Zn with an average 2.6-fold greater accumulation than the control in both of the Zn treatments.

Joint regression was used to explore the interaction between line and Zn exposure in both stem and leaf tissue. The line response to Zn exposure concentration is estimated with the coefficient B1. When B1=1, average stability is indicated and the response of the family is parallel to the

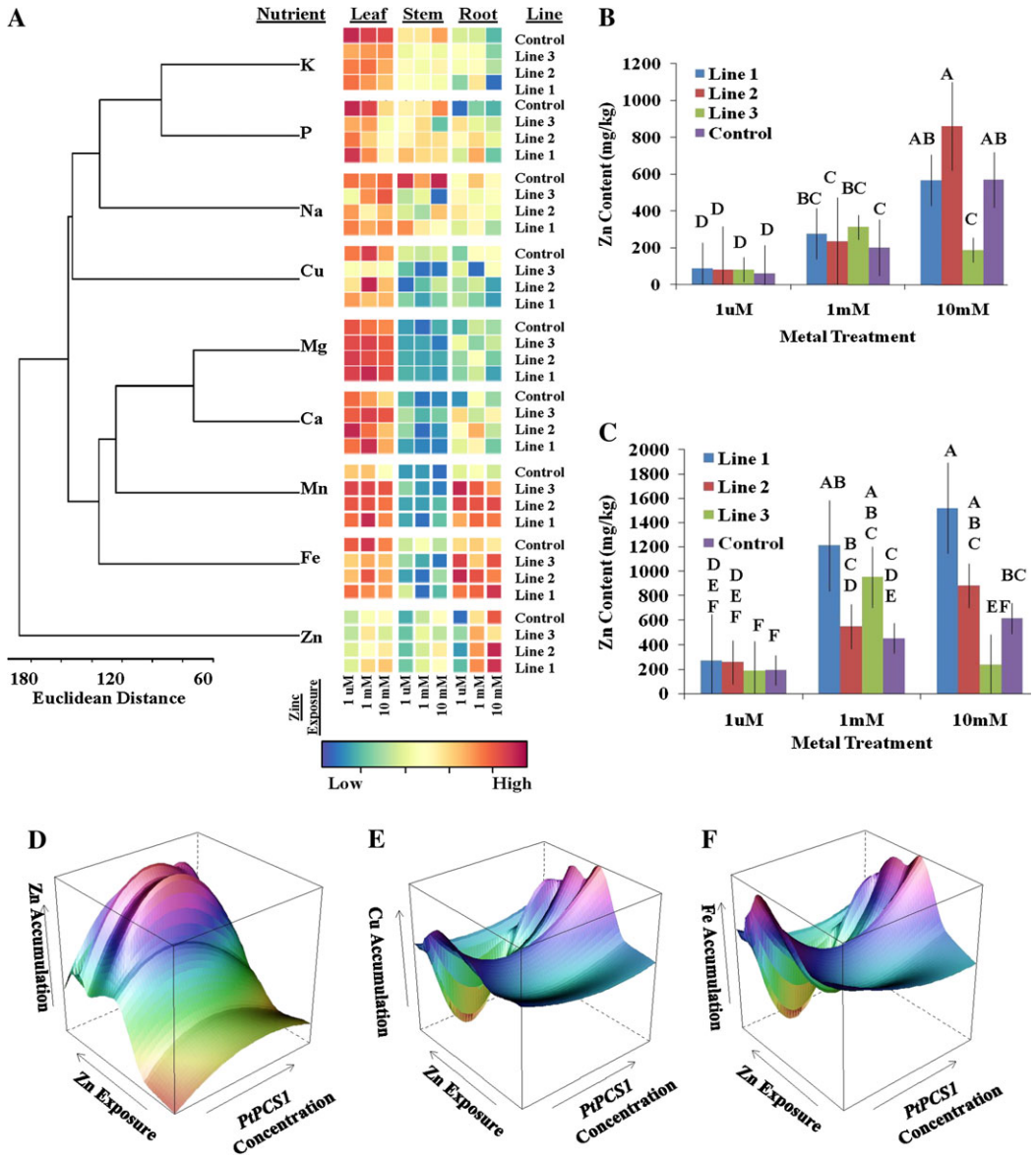

Fig. 5. Nutrient accumulation of P_{35S}:*PtPCS1* lines and control lines (pBI101 and wild-type 717) exposed to 1 μM, 1 mM, or 10 mM Zn (overall n=136). (A) Relationships based on average Euclidian distance of nutrient accumulation across lines, metal exposure, and tissue type and their relative concentrations. Zn accumulation (mg/kg) in stem tissues (B) and leaf tissues (C) across metal treatments, with letters representing least significant difference ranked means within each cluster (metal exposure) while NS represents no difference. Accumulation of (D) Zn, (E) Cu, and (F) Fe in leaf tissue is projected across zinc exposure and *PtPCS1* expression using local regression analysis (model: metal accumulation=*PtPCS1* concentration×metal exposure). In (D), (E), and (F), *PtPCS1* concentration axis represents a range of 0.4–1.2, metal exposure axis represents a range from 0 μM to 10 mM, and Zn, Cu, and Fe accumulation represent ranges 32.5–1521.1, 92.1–732.8, and 4.9–41.6 mg/kg, respectively. Letters in the graph section represent Fisher's PLSD mean separation where differing letters represent significantly different means at the 0.05 level. NS, no significant difference.

response of all families. When B1<1, the family is unresponsive relative to the other families. When B1>1, the family is unstable and exhibits a greater response to Zn exposure concentration than the average response for all families. Relative to the average response of all poplar lines, Line 1 accumulated Zn in stem tissues across the exposure rates at average levels. However, Line 1 accumulated 1.62-fold more than the next highest accumulator (Line 2 in leaves) and accumulated 2.09-fold more Zn than the controls (Supplementary Fig. S1A at *JXB* online). Also Line 1 leaf accumulation was very responsive to the change in exposure concentration (B1=1.43) and increased its accumulation at a greater rate as Zn was added to the system relative to the other tested lines (Supplementary Fig. S1B at *JXB* online). In contrast, Line 3 was less responsive to increased Zn concentrations for both stem and leaf tissues with B1 values 0.50 and 0.86, respectively (Supplementary Fig. S1C at *JXB* online).

Zn accumulation differences are partly explained by the *PtPCS1* levels of each line. Multiple regression using each

line's average *PtPCS1* and *PtHMA4* transcript concentration and Zn exposure level demonstrated that *PtPCS1* and Zn exposure level significantly affected Zn accumulation (P=0.04 and 0.005, respectively) while *PtHMA4* was only influential (P=0.08). Accumulations of other nutrients did not show that they were directly affected by the two transcripts but rather were affected by metal exposure effects. Generally, increased Zn exposure and *PtPCS1* both led to higher Zn accumulation (Fig. 5D). Conversely, the two metal nutrients Cu and Fe, in two differing clusters from Fig. 5A, displayed opposite trends (Fig. 5E, F) with drastic decreases in accumulation as Zn exposure increases, and stability across *PtPCS1* levels.

Discussion

Poplar accumulation of Zn varies clonally (Sebastiani *et al.*, 2004; Laureysens *et al.*, 2005) as do hyperaccumulating species such as *T. caerulescens* (Roosens *et al.*, 2003). Also, poplar is tolerant of sites with increased heavy metal levels, including Zn, but does not accumulate these metals at hyperaccumulator levels of *T. caerulescens.* While genetic variability controlling Zn homeostasis exists in poplar, specific mechanisms are unresolved in this high biomass, forest species. In this study, genomic, transcriptomic, and physiological techniques reveal a coordinated response of *HMA4* and *PCS1* genes through the root and stem to environmental Zn concentrations.

Poplar contains genes with close sequence homology to *HMA4* and *PCS1* implicated in absorption/transport and detoxification of heavy metals in an array of divergent species. In both gene families, all poplar genes are more closely related to the target gene than the monocot rice outgroup consistent with the species phylogeny (Tree of Life; http://tolweb.org/tree). The heavily studied transporter *HMA* family contains 11 potential homologues from poplar and representatives from many other species including hyperaccumulators and non-hyperaccumulators (Fig. 1A). In the *HMA4* family, only one transcript is closely related to *HMA4* members of the Brassicaceae family including those associated with hyperaccumulation. This *HMA4* homologue, *POPTR_0006s07650.1*, is a member of the purported Salicoid duplication gene set (Tuskan *et al.*, 2006). However, its paralogue *POPTR_0018s14140.1* is not in the final phylogenetic tree because of severe truncation (i.e. the protein sequence is only 158 amino acids compared with 1188 amino acids). The *PCS* family only contains two poplar members that are paralogues from the Salicoid duplication event and have diverged from each other greatly compared with paralogues in another non-hyperaccumulator *A. thaliana* (60.4% compared with 70.1% protein sequence identity between paralogues in the respective species) (Heiss *et al.*, 2003). While both genes code for a critical Cys58 residue (Clemens, 2006), only one gene (*POPTR_0014s18420.1*) had many other cysteine motifs (five) conserved across PCS1 from various species.

Because the poplar genome has been duplicated, gene families have expanded in size, nearly doubling the number of *HMA*-like genes and accounting for both *PCS* genes. While poplar has retained many gene paralogues either from a slow evolution rate or not having strong selective pressures for genome downsizing, poplar has not conserved multiple gene copies closely related to those known to be involved in heavy metal hyperaccumulation. This has happened in the hyperaccumulating *A. halleri* where gene expression has been increased by triplication and conservation of HMA4 (Hanikenne *et al.*, 2008) and metal tolerance protein 1 (MTP1; Shahzad *et al.*, 2010).

Poplar down-regulates HMA4 *and* PCS1 *transcripts in response to Zn*

While the poplar genome has maintained *PCS1* and *HMA4* orthologues, its transcriptional control is critical in regulating Zn. Transcripts assayed in this study are both reactive (i.e. root changes correspond to accumulation changes) and proactive (i.e. modulations occur in stems where no accumulation changes have occurred) to environmental Zn demonstrating a tight holistic control of nutrient homeostasis. Transcript modulations contribute to a phenotype in which Zn enters under plant deficiency and is inhibited under surplus. A quick response, within 48 h, of transcriptional abundance occurs in roots and stems even though only roots had significant Zn accumulation differences. Similar tissue coordination of nutrient regulation is seen in the hyperaccumulator *T. caerulescens* for which metal tolerance is associated with stems and hyperaccumulation is associated with roots (de Guimaraes *et al.*, 2009). In roots, *HMA4* and other pathway transcripts related to ATPase-driven transport decrease with the addition of only 10 μM Zn. These same genes, except *ELI-3*, were significantly down-regulated when comparing the non-hyperaccumulating *T. arvense* with the hyperaccumulating *T. caerulescens* (Hammond *et al.*, 2006). None of these genes tested in poplar appeared in the *A. halleri* assay; though this was probably due to the relatively few transcripts that were all up-regulated available from this study (Becher *et al.*, 2004). Decreases observed in poplar and *T. arvense* indicate that transcriptional regulation may be different from that of hyperaccumulators. Poplar, like *A. thaliana*, generally contracts its metal transporter expression as Zn exposure increases (Fig. 2E), keeping localization in roots (Mills *et al.*, 2003; Hussain *et al.*, 2004; Papoyan and Kochian, 2004).

Down-regulation of transporter transcripts is coupled with stable *PtPCS1* expression across the metal gradient and a significant decrease in *PtPCS1* in stems. This corresponds to the tissue compartmentalization seen in *B. juncea* (Heiss *et al.*, 2003) and suggests that PCs are not being used in a traditional detoxification role as proposed by some studies (Clemens *et al.*, 1999; Vatamaniuk *et al.*, 1999; Inouhe *et al.*, 2000; Hartley-Whitaker *et al.*, 2001). Furthermore, *PtPCS1* expression does not correlate with Zn exposure as would be expected if PC production were tightly correlated with glutathione (GSH) increases in poplar leaves (Di Baccio *et al.*, 2005). This may be indicative of a holistic approach employed by poplar in

which down-regulation of PC production in stems may be a method by which PCS physically closer to the point of Zn interaction has adequate GSH for PC production (Cobbett, 2000; Blum *et al.*, 2007),

Altered PtHMA4 *and* PtPCS1 *affect poplar during early development*

Wild-type poplar has *HMA4* and *PCS1* genes that fluctuate with nutrients in a rapid and systemic manner. When these two genes are overexpressed, the genes cause a change in poplar's Zn interacting phenotype. The first major new feature elucidated by these constructs is a positive interaction between the upstream *PCS1* and downstream *HMA4* (Fig. 3C). This link is observed in plants grown at the same low nutrient level; thus, modulations in *HMA4* are most likely not a response to Zn increases but directly related to *PCS1* activity. A functional link between PCS1 and HMA4 has been reported (Fig. 2E) where *A. thaliana* mutants for each gene are additively more sensitive to Cd (Hussain *et al.*, 2004; Wong and Cobbett, 2009), but no previous transcriptional links have been reported.

Gene function is demonstrated by differences in these transgenic lines at early developmental stages. Physiologically, P_{35S}*:PtPCS1* plants were very similar to control plantlets in leaf emergence and days till rooting, while P_{35S}*:PtHMA4* lines were superior (Fig. 3D–G) possibly due to stimulations to the surrounding pathway for ATP production through increased APY2 and AHA3 activity (Fig. 2E) allowing proper cell division, cell growth, and overall plant development (Palmgren and Christensen, 1994; Thomas *et al.*, 1999; Wolf *et al.*, 2007; Wu *et al.*, 2007). P_{35S}*:PtPCS1* rooting percentage was inversely affected by Zn concentration (Fig. 3F) and had overall marginal performance pointing to GSH depletion increasing Zn sensitivity (Gasic and Korban, 2007; Wojas *et al.*, 2008, 2010). As a precursor to other chelation agents, GSH depletion impedes production and function of other metal-interacting proteins such as the *Arabidopsis* oligopeptide transporter (OPT) shutting down meristimatic growth, making plants more sensitive to heavy metals, and halting cell division (Vernoux *et al.*, 2000; Cagnac *et al.*, 2004; Freeman *et al.*, 2005; Blum *et al.*, 2007). This poor performance in the rooting assay illustrates that PCS is functional in poplar but may be an agent for increased absorption and transport efficiency as seen in *A. thaliana*, *Arabidopsis lesbiacum*, and *B. juncea* (Ingle *et al.*, 2005; Bleeker *et al.*, 2006; Gasic and Korban, 2007; Tennstedt *et al.*, 2009).

PtPCS1 *overexpression shifts the poplar phenotype towards an accumulator*

Unlike the drastic negative effects seen in young poplar plants exposed to increased levels of Zn, more mature poplar, with developed roots and leaves, interacts more successfully with Zn even at 10 times the lethal level in the rooting studies. Poplar appears to exert a holistic response to environmental Zn increases by changing physiological processes and nutrient localization. Over 30 d, both P_{35S}*:PtPCS1* lines and controls maintained similar root and stem biomass while leaf biomass increased in controls (Fig. 4A). This may be due to the stable and low control plant TR which allows more leaf surface area since water loss is relatively low (Parker, 1949; Sinclair *et al.*, 2005). Hence, depressed TR may be part of a systematic strategy in which control plants absorb less nutrient solution or compensation for negative impacts on leaf chlorophyll (Ebbs and Uchil, 2008). Furthermore, P_{35S}*:PtPCS1* lines may be better able to maintain normal ion flow across the Zn gradient, preventing K and Na salt build-up in guard cells that could cause increased SR and decreased TR (Dietrich *et al.*, 2001; Brag, 2006).

Complementing the physiological changes, P_{35S}*:PtPCS1* leads to Zn increases in both stem and leaf tissues with a positive relationship between *PCS1* expression levels and the amount of leaf accumulation (Fig. 5B–D). Still the greatest accumulation increases were in the leaves of P_{35S}*:PtPCS1*-Line 1 with an average of 1521 mg/kg in comparison with 30–32 000 mg/kg accumulated by *T. caerulescens* and *A. halleri* under 10 mM and 1 mM Zn treatments, respectively (Brown *et al.*, 1995; Zhao *et al.*, 2000). Though not at hyperaccumulator levels, Line 1 did outperform previous reports from perennial, woody species by achieving leaf Zn concentrations 1.75 times the total applied Zn concentration in the soil after 30 d. This line's accumulation also increased at greater rates than the other lines (B1 coefficient=1.43) shifting this line to an accumulator-like phenotype. Two previous studies involving poplar hybrid and *Salix caprea* accumulated far more Zn in their leaves, but grew on sites with soil concentrations of 47 233 and 14 000 mg kg^{-1}, respectively. These do not approach the relative leaf concentration of Line 1 with concentrations only reaching 7.6% and 33% of the soil concentrations (Pierzynski *et al.*, 2002; Unterbrunner *et al.*, 2007). Since Zn accumulation did not approach concentrations in hyperaccumulating plants, *PCS1* may not be a central contributor to the hyperaccumulating phenotype, possibly due to a broader set of metal-related genes synergistically controlling the wild-type phenotype. This is consistent with recent transformations of *A. thaliana*, in which lines that co-overexpressed both *HMA4* and *MT2b* were significantly more tolerant to Zn and Cd than either single gene overexpression construct (Grispen *et al.*, 2011). Another factor that may inhibit hyperaccumulation is that use of the CaMV 35S promoter provides no tissue localization. This potentially leads to disruption of tissue function, which may be a limiting factor for deducing the true function of a gene such as *PCS1* (Tennstedt *et al.*, 2009; Grispen *et al.*, 2011).

Zn and transcript modulations affect the entire nutrient load

In a broader nutrient scope, poplar accumulates high levels of nutrients in metabolically active tissues such as leaves and, to a lesser extent, roots in both wild-type and transgenic lines (Figs 2A, 5A). The addition of extra Zn into the system affects poplar quickly. After only 48 h, the

highest concentration of Zn-containing solution resulted in a large increase in Zn in roots. This rapid increase in accumulation is at the expense of Cu and Fe, which demonstrate a competitive relationship with Zn. At 48 h, Zn accumulation in leaf and stem tissue was minimal with an ~4-fold and 4.4-fold average decrease relative to accumulation in roots. This trend was accentuated over the longer 30 day assay. As expected, Zn accumulation patterns were different from those of other nutrients. Also, Cu and Fe no longer clustered with Zn after 30 d. Across all tissues, Fe had a net decrease of 9% from the 1 μM Zn to 10 mM Zn levels, which is similar to the antagonistic relationship between these two metals displayed in maize [*Zea mays* (Lee *et al.*, 1969; Rosen *et al.*, 1977; Wang *et al.*, 2009*b*)] associated with competition for the iron/zinc transporters [IRT3/ZNT1 (Cohen *et al.*, 1998; Lombi *et al.*, 2002)]. Alternatively, Cu had a total tissue increase of 28% after 30 d over the 1 μM Zn to 10 mM Zn levels. However, this increase was only found in roots, and in leaf and stems Cu accumulation became increasingly similar to that of Fe (Fig. 5A, E, F). Thus, high Zn is antagonistic to both Cu and Fe at different locations. Fe appears to compete with Zn at the root level, while Cu is unable to transport into the leaves, indicating a possible competitive disadvantage for long-distance transport between the root and stem associated with PCs (Gong *et al.*, 2003; Chen *et al.*, 2006; Mendoza-Cozatl *et al.*, 2008).

In conclusion, poplar growth and development are highly sensitive to environmental Zn at early developmental stages but relatively resilient when tissues are fully differentiated and Zn homeostasis is maintained primarily in roots and leaves where active metabolism is occurring. Poplar seems to have an indicator phenotype providing a systemic, rapid response to changes in Zn availability using *PCS1* and *HMA4* family members. Down-regulation of gene transcriptional abundance generally impedes rapid, long-distance root-to-stem Zn transport in line with reports from other indicator phenotypes. Overexpression of two key genes, *PCS1* and *HMA4*, does alter the phenotype. At early stages of development, *HMA4* relieves some negative effects of Zn, and at later stages metal accumulation is increased by overexpression of *PCS1*. This study elucidated possible avenues of poplar regulation of essential heavy metal accumulation. A still better understanding of the genetic controls used by poplar to interact with heavy metals may be achieved with continued delineation of the larger pathway, inclusion of more expression data from other gene family members, and use of a promoter more consistent with expression localization of hyperaccumulators.

Supplementary data

Supplementay Fig. S1 shows analysis with joint regression of the interaction effects of line–metal treatment of both tissues (stem and leaf).

Supplementary Table S1 lists primers for poplar gene expression analyses via qPCR assays.

Supplementary Table S2 lists primers for poplar gene isolation and restriction site addition with RT-PCR.

Supplementary Table S3 gives gene names, accession numbers, and predicted transmembrane loops/conserved cysteine motifs for respective *HMA4* and *PCS1* genes in the phylogenetic trees.

Supplementary Table S4 shows the pathway connections between treatment and downstream primary and secondary effects.

Supplementary Table S5 shows the relationship between GO annotation groups and pathway gene members.

Supplementary Table S6 lists nutrient averages and variances accumulated in wild-type leaf, stem, and root tissues across metal concentrations at 24 h and 48 h in wild-type plants.

Supplementary Table S7 shows transcription ratio (target gene/ubiquitin) averages and variances across three metal treatments at 24 h and 48 h for root and stem tissues in wild-type plants.

Supplementary Table S8 gives the dry weight averages and variances of PtPCS1 overexpression lines and controls across metal treatments for leaf, stem, and root tissues after 30 d.

Supplementary Table S9 gives nutrient averages and variances accumulated in PtPCS1 overexpression lines and controls in leaf, stem, and root tissues across metal concentrations after 30 d.

Acknowledgements

The authors thank all the student workers who have assisted at various times through the course of this project, most notably L. Vandervelde, M. Monroe, and J. Ellis. They also thank S. Ebbs (Southern Illinois University) and L. Williams (University of Southampton) for providing an external review of this manuscript. This paper was developed under a STAR Research Assistance Agreement No. FP916894 awarded by the Environmental Protection Agency (EPA). It has not been formally reviewed by the EPA. The views expressed in this paper are solely the view of the authors and the EPA does not endorse any products or commercial services mentioned in this paper. This manuscript is number #FO-400 from the Forest and Wildlife Research Center, Mississippi State University.

References

Andres-Colas N, Sancenon V, Rodriguez-Navarro S, Mayo S, Thiele DJ, Ecker JR, Puig S, Penarrubia L. 2006. The *Arabidopsis* heavy metal P-type ATPase HMA5 interacts with metallochaperones and functions in copper detoxification of roots. *The Plant Journal* **45,** 225–236.

Baker AJM. 1981. Accumulators and excluders - strategies in the response of plants to heavy metals. *Journal of Plant Nutrition* **3,** 643–654.

Becher M, Talke IN, Krall L, Kramer U. 2004. Cross-species microarray transcript profiling reveals high constitutive expression of

metal homeostasis genes in shoots of the zinc hyperaccumulator *Arabidopsis halleri*. *The Plant Journal* **37,** 251–268.

Bernard C, Roosens N, Czernic P, Lebrun M, Verbruggen N. 2004. A novel CPx-ATPase from the cadmium hyperaccumulator *Thlaspi caerulescens*. *FEBS Letters* **569,** 140–148.

Bleeker PM, Hakvoort HW, Bliek M, Souer E, Schat H. 2006. Enhanced arsenate reduction by a CDC25-like tyrosine phosphatase explains increased phytochelatin accumulation in arsenate-tolerant *Holcus lanatus*. *The Plant Journal* **45,** 917–929.

Blum R, Beck A, Korte A, Stengel A, Letzel T, Lendzian K, Grill E. 2007. Function of phytochelatin synthase in catabolism of glutathione-conjugates. *The Plant Journal* **49,** 740–749.

Brag H. 2006. The influence of potassium on the transpiration rate and stomatal opening in *Triticum aestivum* and *Pisum sativum*. *Physiologia Plantarum* **26,** 250–257.

Brown S, Chaney R, Angle L, Baker A. 1995. Zinc and cadmium uptake of *T. caerulscens* grown in nutrient solution. *Soil Science Society American Journal* **59,** 125–182.

Cagnac O, Bourbouloux A, Chakrabarty D, Zhang MY, Delrot S. 2004. AtOPT6 transports glutathione derivatives and is induced by primisulfuron. *Plant Physiology* **135,** 1378–1387.

Chaney LR, Brown SL, Li Y-M, *et al*. 2000. Progress in risk assessment for soil metals, and in-situ remediation and phytoextraction of metal from hazardous contaminated soils. *Phytoremediation: State of the science conference*. Boston, MA.

Chen A, Komives EA, Schroeder JI. 2006. An improved grafting technique for mature *Arabidopsis* plants demonstrates long-distance shoot-to-root transport of phytochelatins in *Arabidopsis*. *Plant Physiology* **141,** 108–120.

Clemens S. 2006. Evolution and function of phytochelatin synthases. *Journal of Plant Physiology* **163,** 319–332.

Clemens S, Kim EJ, Neumann D, Schroeder JI. 1999. Tolerance to toxic metals by a gene family of phytochelatin synthases from plants and yeast. *EMBO Journal* **18,** 3325–3333.

Cobbett CS. 2000. Phytochelatins and their roles in heavy metal detoxification. *Plant Physiology* **123,** 825–832.

Cohen CK, Fox TC, Garvin DF, Kochian LV. 1998. The role of iron-deficiency stress responses in stimulating heavy-metal transport in plants. *Plant Physiology* **116,** 1063–1072.

Coleman JE. 1998. Zinc enzymes. *Current Opinion in Chemical Biology* **2,** 222–234.

de Guimaraes MA, Gustin JL, Salt DE. 2009. Reciprocal grafting separates the roles of the root and shoot in zinc hyperaccumulation in *Thlaspi caerulescens*. *New Phytologist* **184,** 323–329.

Di Baccio D, Kopriva S, Sebastiani L, Rennenberg H. 2005. Does glutathione metabolism have a role in the defence of poplar against zinc excess? *New Phytologist* **167,** 73–80.

Dietrich P, Sanders D, Hedrich R. 2001. The role of ion channels in light-dependent stomatal opening. *Journal of Experimental Botany* **52,** 1959–1967.

Ebbs A, Uchil S. 2008. Cadmium and zinc induced chlorosis in Indian mustard [*Brassica juncea* (L.) Czern] involves preferential loss of chlorophyll *b*. *Photosynthetica* **46,** 49–55.

Ebbs SD, Kochian LV. 1998. Phytoextraction of zinc by oat (*Avena sativa*), barley (*Hordeum vulgare*), and Indian mustard (*Brassica juncea*). *Environmental Science and Technology* **32,** 802–806.

Freedman JH, Ciriolo MR, Peisach J. 1989. The role of glutathione in copper metabolism and toxicity. *Journal of Biological Chemistry* **264,** 5598–5605.

Freeman JL, Garcia D, Kim D, Hopf A, Salt DE. 2005. Constitutively elevated salicylic acid signals glutathione-mediated nickel tolerance in *Thlaspi* nickel hyperaccumulators. *Plant Physiology* **137,** 1082–1091.

Gasic K, Korban SS. 2007. Expression of *Arabidopsis* phytochelatin synthase in Indian mustard (*Brassica juncea*) plants enhances tolerance for Cd and Zn. *Planta* **225,** 1277–1285.

Gong JM, Lee DA, Schroeder JI. 2003. Long-distance root-to-shoot transport of phytochelatins and cadmium in *Arabidopsis*. *Proceedings of the National Academy of Sciences, USA* **100,** 10118–10123.

Grill E, Winnacker EL, Zenk MH. 1985. Phytochelatins: the principal heavy-metal complexing peptides of higher plants. *Science* **230,** 674–676.

Grispen VMJ, Hakvoort HWJ, Bliek T, Verkleij JAC, Schat H. 2011. Combined expression of the *Arabidopsis* metallothionein MT2b and the heavy metal transporting ATPase HMA4 enhances cadmium tolerance and the root to shoot translocation of cadmium and zinc in tobacco. *Envionmental and Experimental Botany* .

Hammond JP, Bowen HC, White PJ, Mills V, Pyke KA, Baker AJ, Whiting SN, May ST, Broadley MR. 2006. A comparison of the *Thlaspi caerulescens* and *Thlaspi arvense* shoot transcriptomes. *New Phytologist* **170,** 239–260.

Han K-H, Meilan R, Ma C, Strauss SH. 2000. An *Agrobacterium tumefaciens* transformation protocol effective on variety of cottonwood hybrids (genus *Populus*). *Plant Cell Reports* **19,** 315–320.

Hanikenne M, Talke IN, Haydon MJ, Lanz C, Nolte A, Motte P, Kroymann J, Weigel D, Kramer U. 2008. Evolution of metal hyperaccumulation required cis-regulatory changes and triplication of HMA4. *Nature* **453,** 391–395.

Hartley-Whitaker J, Ainsworth G, Vooijs R, Ten Bookum W, Schat H, Meharg AA. 2001. Phytochelatins are involved in differential arsenate tolerance in *Holcus lanatus*. *Plant Physiology* **126,** 299–306.

Hartwig A, Asmuss M, Ehleben I, Herzer U, Kostelac D, Pelzer A, Schwerdtle T, Burkle A. 2002. Interference by toxic metal ions with DNA repair processes and cell cycle control: molecular mechanisms. *Environmental Health Perspectives* **110,** Suppl. 5, 797–799.

Heiss S, Wachter A, Bogs J, Cobbett C, Rausch T. 2003. Phytochelatin synthase (PCS) protein is induced in *Brassica juncea* leaves after prolonged Cd exposure. *Journal of Experimental Botany* **54,** 1833–1839.

Hussain D, Haydon MJ, Wang Y, Wong E, Sherson SM, Young J, Camakaris J, Harper JF, Cobbett CS. 2004. P-type ATPase heavy metal transporters with roles in essential zinc homeostasis in *Arabidopsis*. *The Plant Cell* **16,** 1327–1339.

Infante C, Matsuoka MP, Asensio E, Canavate JP, Reith M, Manchado M. 2008. Selection of housekeeping genes for gene

expression studies in larvae from flatfish using real-time PCR. *BMC Molecular Biology* **9,** 28.

Ingle RA, Mugford ST, Rees JD, Campbell MM, Smith JA. 2005. Constitutively high expression of the histidine biosynthetic pathway contributes to nickel tolerance in hyperaccumulator plants. *The Plant Cell* **17,** 2089–2106.

Inouhe M, Ito R, Ito S, Sasada N, Tohoyama H, Joho M. 2000. Azuki bean cells are hypersensitive to cadmium and do not synthesize phytochelatins. *Plant Physiology* **123,** 1029–1036.

Isaac RA. 1983. *Reference soil test methods for the southern region of the United States*. Southern Cooperative Series Bulletin 289: Athens, GA.

Kohler A, Blaudez D, Chalot M, Martin F. 2004. Cloning and expression of multiple metallothioneins from hybrid poplar. *New Phytologist* **164,** 83–93.

Lasat MM, Baker AJ, Kochian LV. 1998. Altered Zn compartmentation in the root symplasm and stimulated Zn absorption into the leaf as mechanisms involved in Zn hyperaccumulation in *Thlaspi caerulescens*. *Plant Physiology* **118,** 875–883.

Laureysens I, De Temmerman L, Hastir T, Van Gysel M, Ceulemans R. 2005. Clonal variation in heavy metal accumulation and biomass production in a poplar coppice culture. II. Vertical distribution and phytoextraction potential. *Environmental Pollution* **133,** 541–551.

Lee CR, Craddock GR, Hammer HE. 1969. Factors affecting plant growth in high zinc medium: I. Influence of iron on growth of flax at various zinc levels. *Agronomy Journal* **61,** 562–565.

Lombi E, Tearall KL, Howarth JR, Zhao FJ, Hawkesford MJ, McGrath SP. 2002. Influence of iron status on cadmium and zinc uptake by different ecotypes of the hyperaccumulator *Thlaspi caerulescens*. *Plant Physiology* **128,** 1359–1367.

Long XX, Yang XE, Ni WZ, Ye ZQ, He ZL, Calvert DV, Stoffella JP. 2003. Assessing zinc thresholds for phytotoxicity and potential dietary toxicity in selected vegetable crops. *Communications in Soil Science and Plant Analysis* **24,** 1412–1434.

Mendoza-Cozatl DG, Butko E, Springer F, Torpey JW, Komives EA, Kehr J, Schroeder JI. 2008. Identification of high levels of phytochelatins, glutathione and cadmium in the phloem sap of *Brassica napus*. A role for thiol-peptides in the long-distance transport of cadmium and the effect of cadmium on iron translocation. *The Plant Journal* **54,** 249–259.

Michaelis A, Takehisa RS, Reiger R, Aurich O. 1986. Ammonium chloride and zinc sulfate pretreatments reduce the yield of chromatid aberrations induced by TEM and maleic hydrazide in *Vicia faba*. *Mutation Research* **173,** 187–191.

Mills RF, Krijger GC, Baccarini PJ, Hall JL, Williams LE. 2003. Functional expression of AtHMA4, a P1B-type ATPase of the Zn/Co/Cd/Pb subclass. *The Plant Journal* **35,** 164–176.

Palmgren MG, Christensen G. 1994. Functional comparisons between plant plasma membrane H(+)-ATPase isoforms expressed in yeast. *Journal of Biological Chemistry* **269,** 3027–3033.

Papoyan A, Kochian LV. 2004. Identification of *Thlaspi caerulescens* genes that may be involved in heavy metal hyperaccumulation and tolerance. Characterization of a novel heavy metal transporting ATPase. *Plant Physiology* **136,** 3814–3823.

Parker J. 1949. Effects of variations in the root-leaf ratio on transpiration rate. *Plant Physiology* **24,** 739–743.

Pierzynski GM, Schoor JL, Yougman A, Licht L, Erickson LE. 2002. Poplar trees for phytostabilization of abandoned zinc-lead smelter. *Practice Periodical of Hazardous, Toxic, and Radioactive Waste Management* **6,** 177–183.

R Development Core Team. 2008. *R: A language and environment for statistical computing*. Vienna, Austria: R Foundation for Statistical Computing.

Roosens N, Verbruggen N, Meerts P, Ximenez-Embun P, Smith JAC. 2003. Natural variation in cadmium tolerance and its relationship to metal hyperaccumulation for seven populations of *Thlaspi caerulescens* from western Europe. *Plant, Cell and Environment* **26,** 1657–1672.

Rosen JA, Pike CS, Golden ML. 1977. Zinc, iron, and chlorophyll metabolism in zinc-toxic corn. *Plant Physiology* **59,** 1085–1087.

Sebastiani L, Francesca S, Tognetti R. 2004. Heavy metal accumulation and growth responses in poplar clones Eridano (*Populus deltoides*×*maximowiczii*) and I-214 (*P.*×*euramericanca*) exposed to industrial waste. *Environmental and Experimental Botany* **52,** 79–88.

Shahzad Z, Gosti F, Frerot H, Lacombe E, Roosens N, Saumitou-Laprade P, Berthomieu P. 2010. The five AhMTP1 zinc transporters undergo different evolutionary fates towards adaptive evolution to zinc tolerance in *Arabidopsis halleri*. *PLoS Genetics* **6,** e1000911.

Sinclair TR, Holbrook NM, Zwieniecki MA. 2005. Daily transpiration rates of woody species on drying soil. *Tree Physiology* **25,** 1469–1472.

Tamura K, Dudley J, Nei M, Kumar S. 2007. MEGA4: molecular evolutionary genetics analysis (MEGA) software version 4.0. *Molecular Biology and Evolution* **24,** 1596–1599.

Tennstedt P, Peisker D, Bottcher C, Trampczynska A, Clemens S. 2009. Phytochelatin synthesis is essential for the detoxification of excess zinc and contributes significantly to the accumulation of zinc. *Plant Physiology* **149,** 938–948.

Thomas C, Sun Y, Naus K, Lloyd A, Roux S. 1999. Apyrase functions in plant phosphate nutrition and mobilizes phosphate from extracellular ATP. *Plant Physiology* **119,** 543–552.

Thompson JD, Gibson TJ, Plewniak F, Jeanmougin F, Higgins DG. 1997. The CLUSTAL_X windows interface: flexible strategies for multiple sequence alignment aided by quality analysis tools. *Nucleic Acids Research* **25,** 4876–4882.

Tuskan GA, Difazio S, Jansson S, *et al*. 2006. The genome of black cottonwood, *Populus trichocarpa* (Torr. & Gray). *Science* **313,** 1596–1604.

Tusnady GE, Simon I. 1998. Principles governing amino acid composition of integral membrane proteins: application to topology prediction. *Journal of Molecular Biology* **283,** 489–506.

Unterbrunner R, Puschenreiter M, Sommer P, Wieshammer G, Tlustos P, Zupan M, Wenzel WW. 2007. Heavy metal accumulation in trees growing on contaminated sites in Central Europe. *Environmental Pollution* **148,** 107–114.

Vallee BJ, Falchuk H. 1993. The biochemical basis of zinc physiology. *Physiological Reviews* **73,** 79–118.

Vatamaniuk OK, Mari S, Lu YP, Rea PA. 1999. AtPCS1, a phytochelatin synthase from *Arabidopsis*: isolation and in vitro reconstitution. *Proceedings of the National Academy of Sciences, USA* **96,** 7110–7115.

Vernoux T, Wilson RC, Seeley KA, *et al*. 2000. The ROOT MERISTEMLESS1/CADMIUM SENSITIVE2 gene defines a glutathione-dependent pathway involved in initiation and maintenance of cell division during postembryonic root development. *The Plant Cell* **12,** 97–110.

Wan C-Y, Wilkins TA. 1994. A modified hot borate method significantly enhances the yield of high-quality RNA from cotton (*Gossypium hirsutum* L.). *Analytical Biochemistry* **233,** 7–12.

Wang C, Zhang SH, Wang PF, Hou J, Zhang WJ, Li W, Lin ZP. 2009 *a*. The effect of excess Zn on mineral nutrition and antioxidative response in rapeseed seedlings. *Chemosphere* **75,** 1468–1476.

Wang Z, Fu Z, Ye C. 2009 *b*. Recovery of nickel from aqueous samples with water-soluble carboxyl methyl cellulose-acetone system. *Journal of Hazardous Materials* **170,** 705–710.

Wei S, Zhou Q, Wang X. 2005. Identification of weed plants excluding the uptake of heavy metals. *Environmental International* **31,** 829–834.

Wenzel WW, Bunkowski M, Puschenreiter M, Horak O. 2003. Rhizosphere characteristics of indigenously growing nickel hyperaccumulator and excluder plants on serpentine soil. *Environmental Pollution* **123,** 131–138.

Wojas S, Clemens S, Hennig J, Sklodowska A, Kopera E, Schat H, Bal W, Antosiewicz DM. 2008. Overexpression of phytochelatin synthase in tobacco: distinctive effects of AtPCS1 and CePCS genes on plant response to cadmium. *Journal of Experimental Botany* **59,** 2205–2219.

Wojas S, Clemens S, Sklodowska A, Maria Antosiewicz D. 2010. Arsenic response of AtPCS1- and CePCS-expressing plants - effects of external As(V) concentration on As-accumulation pattern and NPT metabolism. *Journal of Plant Physiology* **167,** 169–175.

Wolf C, Hennig M, Romanovicz D, Steinebrunner I. 2007. Developmental defects and seedling lethality in apyrase AtAPY1 and AtAPY2 double knockout mutants. *Plant Molecular Biology* **64,** 657–672.

Wong CK, Cobbett CS. 2009. HMA P-type ATPases are the major mechanism for root-to-shoot Cd translocation in *Arabidopsis thaliana*. *New phytologist* **181,** 71–78.

Wu J, Steinebrunner I, Sun Y, Butterfield T, Torres J, Arnold D, Gonzalez A, Jacob F, Reichler S, Roux SJ. 2007. Apyrases (nucleoside triphosphate-diphosphohydrolases) play a key role in growth control in *Arabidopsis*. *Plant Physiology* **144,** 961–975.

Zhao FJ, Lombi E, Breedon T, McGrath SP. 2000. Zinc hyperaccumulation and cellular disruption in *Arabidopsis halleri*. *Plant, Cell and Environment* **23,** 507–514.